Received: 19 October 2021 | Accepted: 23 November 2021

DOI: 10.1111/1759-7714.14264

ORIGINAL ARTICLE

WILEY

CircRNA PRH1-PRR4 stimulates RAB3D to regulate the malignant progression of NSCLC by sponging miR-877-5p

Jun Ma[1] | **Quanxing Li**[2] | **Yuling Li**[3]

[1]Department of Respiratory and Critical Care Medicine, Dongying People's Hospital, Dongying City, 257000, Shandong, China

[2]Department of Cardiothoracic Surgery, Dongying People's Hospital, Dongying City, 257000, Shandong, China

[3]Department of Respiratory and Critical Care Medicine, Tengzhou Central People's Hospital, Tengzhou Ctiy, 277500, Shandong, China

Correspondence
Quanxing Li, Department of Cardiothoracic Surgery, Dongying People's Hospital, No. 238, South 1st Road, Dongcheng Street, Dongying District, Dongying City, 257000, China.
Email: zabnaf@163.com

Abstract

Background: Previous reports have confirmed the importance of circular RNA (circRNA) in the malignant progression of non-small-cell lung cancer (NSCLC). However, the role of circRNA PRH1-PRR4 readthrough (circPRH1-PRR4) in NSCLC progression was unclear. This study was designed to reveal the mechanism behind circPRH1-PRR4 regulating NSCLC progression.

Methods: Quantitative real-time polymerase chain reaction and western blot were employed to detect the expression of circPRH1-PRR4, microRNA-877-5p (miR-877-5p), the member RAS oncogene family (RAB3D), and other indicated protein markers. The positive expression rate of RAB3D was detected by immunohistochemistry assay. Cell proliferation was investigated by cell colony formation and 5-ethynyl-2′-deoxyuridine assays. Flow cytometry was employed to quantify apoptotic cells. Wound-healing and transwell invasion assays were used to evaluate cell metastasis. The interaction among circPRH1-PRR4, miR-877-5p, and RAB3D was identified by dual-luciferase reporter assay. In vivo assay was implemented to demonstrate the effect of circPRH1-PRR4 on tumor formation.

Results: As compared with controls, NSCLC tissues and cells displayed high expression of circPRH1-PRR4 and RAB3D, and low expression of miR-877-5p. Reduced expression of circPRH1-PRR4 resulted in inhibition of cell proliferation, migration, and invasion, but promotion of cell apoptosis in vitro. In support, circPRH1-PRR4 silencing inhibited tumor formation in vivo. Knockdown of miR-877-5p, a target miRNA of circPRH1-PRR4, relieved circPRH1-PRR4 absence-mediated action. Additionally, RAB3D was identified as a target mRNA of miR-877-5p. Importantly, circPRH1-PRR4 regulated RAB3D expression by miR-877-5p.

Conclusion: CircPRH1-PRR4 knockdown impeded NSCLC cell malignancy by the miR-877-5p/RAB3D pathway, providing a possible circRNA-targeted therapy for NSCLC.

KEYWORDS
circPRH1-PRR4, miR-877-5p, NSCLC, RAB3D

INTRODUCTION

As the main killers of cancer-associated death worldwide, lung cancer has gradually become a deadly threat to people's health.[1] About 85% of total lung carcinomas are identified as non-small-cell lung cancer (NSCLC).[2] The conventional therapeutic method for NSCLC cases is a combination of surgical resection and chemotherapy; however, the clinical outcomes of NSCLC sufferers are still poor because of frequent metastasis and recurrence.[3] Thus, an in-depth investigation about the pathophysiological mechanisms behind NSCLC progression and reliable targets for promoting the prediction of therapeutic outcome is beneficial for the therapy and diagnosis of NSCLC.

Jun Ma and Quanxing Li contributed equally to this work.

Circular RNA (circRNA) is a conserved endogenous molecule with a covalently closed cyclic structure formed from the abnormal spicing of linear premessenger RNA.[4] The special circular structure makes circRNA able to resist RNase-caused degradation. On that account, circRNA is more stable than the linear gene, and thereby can be employed as a diagnostic or therapeutic biomarker of cancers.[5] CircRNA can sink for microRNA (miRNA) to regulate the function induced by miRNA.[6] Additionally, circRNA modulates the target gene level through interaction with RNA-binding proteins.[7] Through the experimental explanations of its protumoral and tumor-repressing features, circRNA is identified as a key molecule in the development of various cancers, including NSCLC.[8] CircRNA PRH1-PRR4 readthrough (circPRH1-PRR4), only named as circ_0000376 and circ_000554, has been validated as an oncogene by binding to miR-145-5p in gastric cancer[9] and a tumor suppressor through trapping miR-182 in breast cancer.[10] Unfortunately, the working mechanism of the circRNA in NSCLC progression is under-reported.

As another noncoding RNA, miRNA contains 18–24 nucleotides and is regulated by circRNA in a competing endogenous RNA (ceRNA)-dependent way.[11] In addition, miRNA can bind to the noncoding region of the target gene, leading to translation inhibition or mRNA degradation.[12] Increasing studies have unveiled the importance of miRNA in NSCLC malignant progression. For instance, miR-7-5p inhibited metastasis of NSCLC cells via interacting with neuro-oncological ventral antigen 2 (NOVA2).[13] MiR-145-5p hindered cell proliferation and immune evasion by negatively regulating C-X-C motif chemokine ligand 3 (CXCL3).[14] On the contrary, miR-761 acted as a promoter in NSCLC cell malignancy by regulating cell proliferation and aggressiveness.[15] Given the feasibility of the circRNA-miRNA-mRNA regulatory network in revealing the mechanism responsible for cancer progression,[16,17] we predicted the miRNA and mRNA associated with circPRH1-PRR4 through bioinformatics tools. As a result, we found miR-877-5p was able to bind to circPRH1-PRR4, and the member RAS oncogene family (RAB3D) carried the complementary sites of miR-877-5p. Hence, the circPRH1-PRR4-miR-877-5p-RAB3D interaction network was explored in NSCLC.

This study checked circPRH1-PRR4 expression in NSCLC tissues and cells, and explored the role of circPRH1-PRR4 in NSCLC cell malignancy. Additionally, whether or not circPRH1-PRR4-miR-877-5p-RAB3D network was responsible for NSCLC progression was determined.

MATERIALS AND METHODS

Clinical NSCLC samples

With the approval of the Ethics Committee of Dongying People's Hospital, 33 pairs of NSCLC tissues and matched healthy lung tissues were collected from NSCLC patients who completed surgical operations in Dongying People's Hospital. Immediately after operation, these tissues were stored at −80°C. Radiation therapy or chemotherapy was not performed on these sufferers. Each subject signed the written informed consent.

Cell culture

NSCLC cell-lines A549 and H522, and human normal lung epithelial cell (BEAS-2B) were purchased from Procell or EK-Bioscience. A549 cells were maintained in Ham's F12K (Procell), and H522 and BEAS-2B were grown at the Roswell Park Memorial Institute-1640 (RPMI-1640; Procell) at 37°C in an incubator containing 5% CO_2. In particular, the media were supplemented with 10% fetal bovine serum (FBS; Procell) as well as 1% penicillin/streptomycin (Millipore).

Cell transfection

According to the manufacturer's instructions, cell transfection was conducted using jetPRIME or INTERFERin (Polyplus-transfection). In brief, A549 and H522 cells at ∼70% confluence in 12-well plates were treated with 50 nM of miRNA mimics and siRNAs, 100 nM of miRNA inhibitors, and 2 μg of plasmids or matched controls, followed by incubation for 48 h. The plasmids and oligonucleotides used were built by GenePharma and are as follows: the small interfering RNAs against circPRH1-PRR4 (si-circPRH1-PRR4#1, 5′-TCCATATGA GAGTTGGATTCT-3′; si-circPRH1-PRR4#2, 5′-TATCCATAT GAGAGTTGGATT-3′), the mimics and inhibitors of miR-877-5p (miR-877-5p mimic 5′-GUAGAGGAGAUGGC GCAGGG-3′; miR-877-5p inhibitor 5′-CCCUGCGCCAUCUC CUCUAC-3′), the plasmid overexpressing RAB3D (pcDNA-RAB3D), and respective controls (si-NC, sh-NC, miR-NC mimic, miR-NC inhibitor and pcDNA-NC).

Lentivirus stable transduction

The small hairpin RNA specific to circPRH1-PRR4 (sh-circPRH1-PRR4 5′-TCCATATGAGAGTTGGATTCT-3′) and matched controls (sh-NC) were established using LV3-CMV-GFP-Puro vector (GenePharma). Cell transfection was carried out and cells were allowed to grow for 24 h. Then, 2 μg/ml puromycin (Sigma) was used to select stably infected cells. After 1 week, the successfully reduced expression of circPRH1-PRR4 was determined by quantitative real-time polymerase chain reaction (qRT-PCR). The lentivirus used to overexpress RAB3D or decrease miR-877-5p in NSCLL cells was provided by GenePharma.

Quantitative real-time polymerase chain reaction

Based on the standard instructions, TransZol (TransGen) was used to isolate RNA from each specimen and cell. The quality assurance of isolated RNA was confirmed by

TABLE 1 The sequences of forward and reverse primers used in this research

Gene	Sequences of primers (from 5′ to 3′)
circPRH1-PRR4-F	AGGCTAGTTTGGATGTGG
circPRH1-PRR4-R	AGGTGGGAGGATGGTTTG
PRH1-PRR4-F	GGGGCAGTCTCCTCAGTAAT
PRH1-PRR4-R	ACCAGGGGGTCTAGGTAGGA
miR-877-5p-F	GCCGTAGAGGAGATGGC
miR-877-5p-R	CAGTGCGTGTCGTGGA
RAB3D-F	ATGGACTGTGATCAGTGCCG
RAB3D-R	AGCAAAGAAAAGGTGCTGCG
β-actin-F	CACCATTGGCAATGAGCGGTTC
β-actin-R	AGGTCTTTGCGGATGTCCACGT
U6-F	CTCGCTTCGGCAGCACA
U6-R	AACGCTTCACGAATTTGCGT

evaluating the ratio of absorbance at 260 (A260)/A280. Reaction reagents containing 50 ng to 2 μg total RNA were employed for the synthesis of cDNA by using commercial cDNA synthesize kits (Thermo Fisher). Gene expression was analyzed using a qRT-PCR SuperMix (Corning) on a Bio-Rad 96-well plate (Hercules), and calculated with the $2^{-\Delta\Delta Ct}$ method. The qRT-PCR was cycled at 95°C for 60 s, 40 cycles at 95°C for 5 s, and 60°C for 15 s. The primers are listed in Table 1. U6 and β-actin were utilized to normalize gene expression.

Identification of circRNA stability

One microgram of RNA was employed to incubate with RNase R (Geneseed) at 37°C to identify the stability of circPRH1-PRR4. The same content of RNA not incubated with RNase R was used as a control (Mock). Finally, the expression of circPRH1-PRR4 and PRH1-PRR4 was determined by qRT-PCR.

Cell colony formation assay

H522 and A549 cells were inoculated into cell culture dish (500 cells per hole). After transfection of test compounds, including si-circPRH1-PRR4, miR-877-5p mimic, miR-877-5p inhibitor, pcDNA-RAB3D, si-NC, miR-NC mimic, miR-NC inhibitor, and pcDNA-NC, the cells were allowed to grow for about 10 days. Afterwards, methanol and crystal violet purchased from Phygene were used to fix and dye cells, respectively. Lastly, the number of the colonies greater than 1 mm in diameter was counted.

5-Ethynyl-2′-deoxyuridine assay

H522 and A549 cells were seeded in 12-well plates (1×10^5 cells per well) and transfected with plasmids or oligonucleotides. Forty-eight hours later, the cells were passaged in the microplates, which was pre-incubated with 50 μM 5-ethynyl-2′-deoxyuridine (EdU)-labeled medium for 2 h. Then, cell proliferation was evaluated using an EdU staining kit (Ribobio) as per the manufacturer's recommendations. Cell nuclei were stained by 4′,6-diamidino-2-phenylindole (DAPI; Phygene). A fluorescence microscope (Olympus) was used to observe EdU-positive cells.

Cell apoptosis

An Annexin V-FITC apoptosis detection kit (Dojindo) was used. Briefly, the cells transfected with test compounds were allowed to grow for 48 h and harvested by centrifugation. Then, Annexin V Binding Solution was used to suspend the cells, which were subsequently incubated with mixtures of Annexin V-FITC and propidium iodide (PI) for 15 min in the dark. Finally, a flow cytometer (Thermo Fisher) was utilized to quantify apoptotic cells.

Wound-healing assay

After the treatment, NSCLC cells were grown in six-well plates with Ham's F12K or RPMI-1640 at a confluence of 2×10^5 cells per well until they reached ∼90% confluence. Then, floated cells and debris were removed and a single-cell layer was created using 10-μl pipette tips. After performing cell culture for 24 h, the width of the scratch gap was measured under a low-power (40×) microscope (Olympus).

Transwell invasion assay

The 1×10^5 cells transfected with plasmids or oligonucleotides were diluted in serum-free Ham's F12K or RPMI-1640 (Procell) and added into the upper inserts precoated with 100 μl of Matrigel (Corning), while the same number of cells was plated in the lower inserts supplemented with media containing 15% FBS (Procell). After 24 h of incubation, methanol and crystal violet (Phygene) were utilized to fix and stain the cells adhering to the top surface of the lower inserts. Finally, the cells from six representative fields were quantified using a high-power (100×) microscope (Olympus).

Western blot analysis

Total proteins were extracted using a protein extraction kit (Phygene). A BCA Protein Assay Kit (Phygene) was used to quantify the concentration of protein. After proteins were denatured at 95°C for 10 min, a Tricine-SDS-PAGE Gel Kit (Phygene) was used to prepare the SDS-PAGE gels separating protein bands. The proteins were transferred onto nitrocellulose membranes (Roche) and immersed in 5% defatted dry milk to block aspecific signals. The membranes were

incubated with anti-matrix metalloprotein 2 (anti-MMP2, 1:2000; Cusabio Biotech), anti-MMP9 (1:800; Cusabio Biotech), anti-RAB3D (1:1000; Affinity), and anti-β-actin (1:5000; Affinity). Subsequently, the membranes were washed using Tris buffered saline Tween (Millipore) and incubated with horseradish peroxidase-labeled secondary antibody (1:5000; Affinity). Biuret Reagent (A + B) (Phygene) was used to develop protein blots. β-actin served as a control.

Dual-luciferase reporter assay

Prediction websites (https://circinteractome.nia.nih.gov/index.html and http://starbase.sysu.edu.cn/agoClipRNA.php?source=mRNA) were used to demonstrate whether miR-877-5p was able to bind to circPRH1-PRR4 and RAB3D. Based on the possible binding sites of miR-877-5p and circPRH1-PRR4 or RAB3D, the wild-type (WT) vectors (WT-circPRH1-PRR4 and WT-RAB3D 3′UTR) were created by GeneCopoeia by using the sequences of circPRH1-PRR4 and RAB3D 3′-untranslated regions (3′UTRs) harboring the binding sites of miR-877-5p. The complementary sites of circPRH1-PRR4 and RAB3D with miR-877-5p were mutated using a site-directed mutation kit (Yeasen) and used to build the mutant plasmids, including MUT-circPRH1-PRR4 and MUT-RAB3D 3′UTR. Subsequently, NSCLC cells seeded in 24-well plates were treated with the above plasmids, miR-877-5p mimic or miR-NC mimic using jetPRIME or INTERFERin (Polyplus-transfection). Forty-eight hours later, fluorescence signals were detected using a Dual-Lucy Assay Kit (Solarbio). The binding intensity was confirmed by assessing the ratio of *firefly* luciferase activity to *Renilla* luciferase activity.

In vivo experiment

The lentivirus expressing sh-circPRH1-PRR4 and the lentivirus expressing sh-NC were designed and packaged by FulenGen using a LV3-CMV-GFP-Puro vector. The xenograft mouse model assay was performed on 12 4–6-week-old male BALB/c nude mice (Charles River) under the agreement of the Animal Care and Use Committee of Dongying People's Hospital. All these mice were assigned to two groups: (1) a sh-circPRH1-PRR4 group (treated with 5×10^6 A549 cells expressing sh-circPRH1-PRR4) or (2) a sh-NC group (injected with 5×10^6 A549 cells expressing sh-NC). The cells infected with the lentivirus were subcutaneously injected into the dorsal side of the mice. The length (L) and width (W) of the forming tumors were measured every 7 days from the seventh day after injection. Thirty-five days later, all mice were euthanatized using xylazine (10 mg/kg). The neoplasms were harvested to assess tumor weight and gene expression. The volume (V) of the nodules was calculated according to the formula: $V\ (\mathrm{mm}^3) = W^2 \times L \times 0.5$.

Immunohistochemistry assay

Positive expression rate of RAB3D was presented by immunohistochemistry (IHC) assay based on previous methods [18]. In short, paraffin-embedded tissues were cut into 4-μm

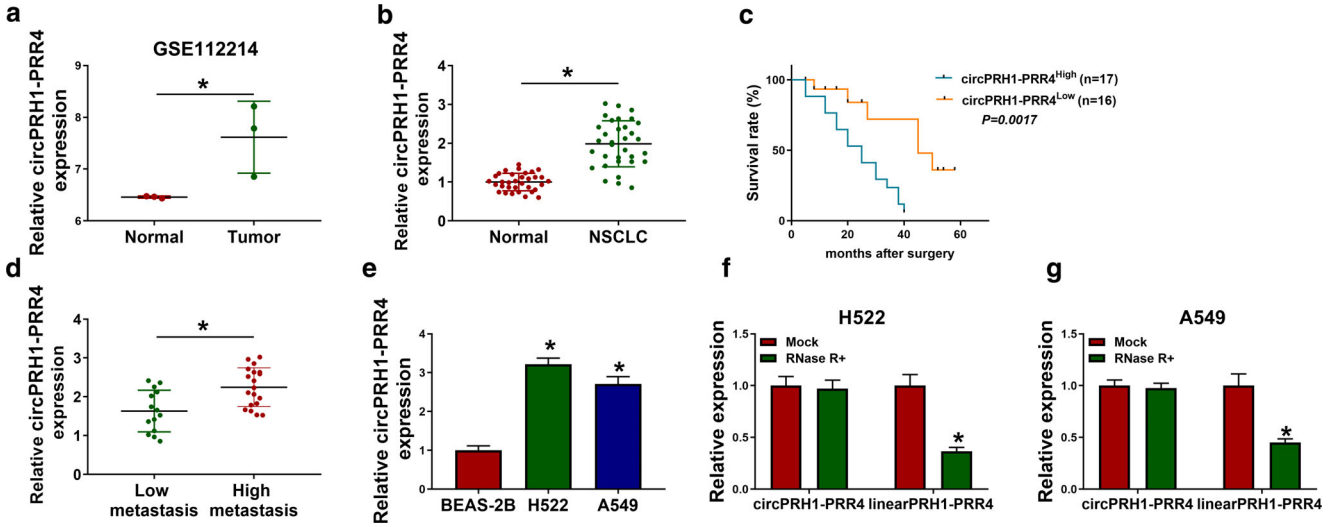

FIGURE 1 The expression of circPRH1-PRR4 in NSCLC tissues and cells. (a) CircPRH1-PRR4 expression was identified by using the GSE112214 dataset. (b and e) CircPRH1-PRR4 expression was detected by qRT-PCR in clinical NSCLC tissues ($N = 33$), healthy lung tissues ($N = 33$) as well as BEAS-2B, H522 and A549 cells. (c) Kaplan–Meier method was used to analyze overall survival curve of NSCLC patients with high or low circPRH1-PRR4 expression. (d) The expression of circPRH1-PRR4 was detected by qRT-PCR in high-metastatic NSCLC tissues ($N = 19$) and low-metastatic NSCLC tissues ($N = 14$). (f and g) RNase R treatment assay was employed to identify the stability of circPRH1-PRR4. The low and high expressions of circPRH1-PRR4 were divided with the mean expression of circPRH1-PRR4 as the cut-off value. $^*p < 0.05$

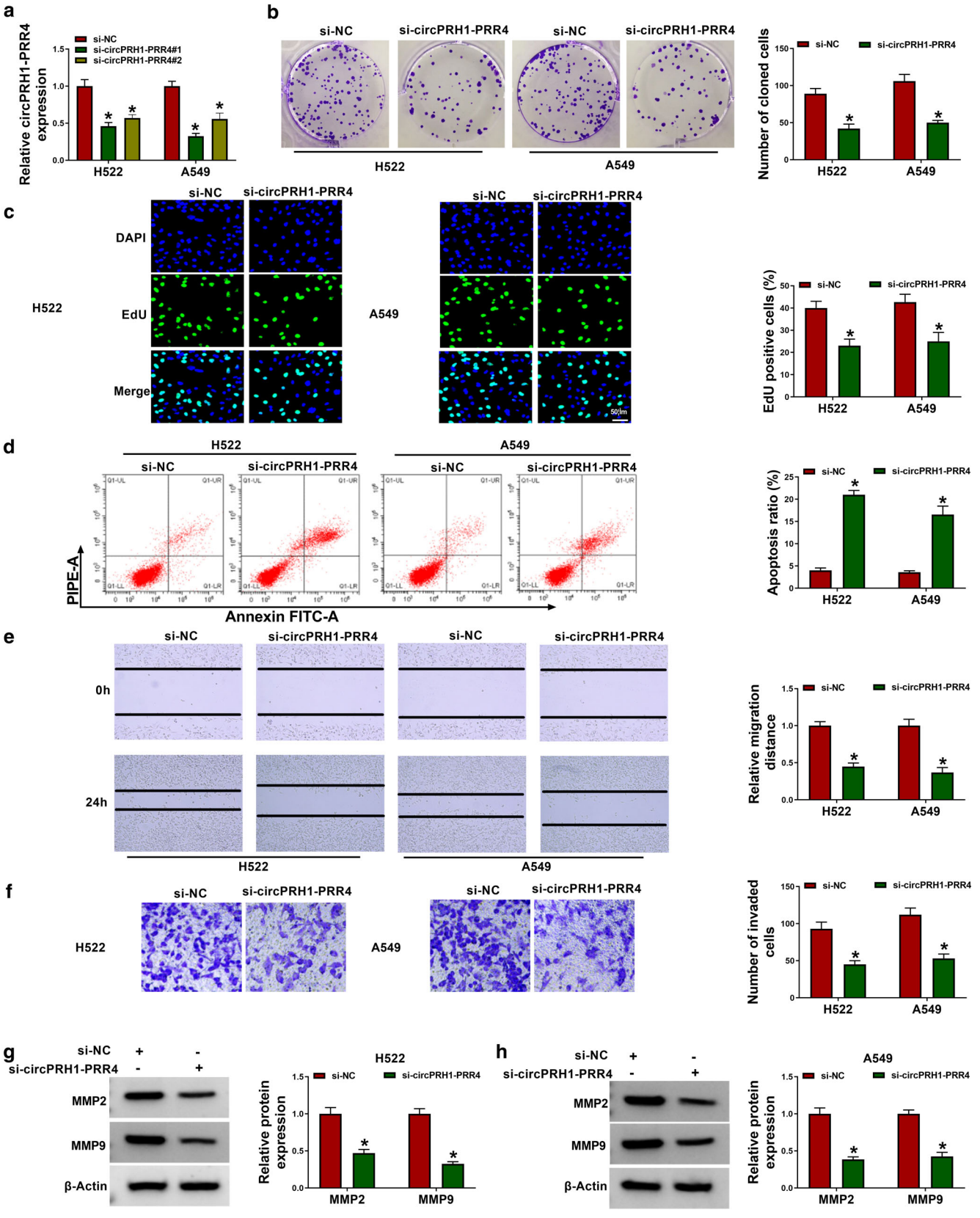

FIGURE 2 Effects of circPRH1-PRR4 silencing on NSCLC cell processes. (a) CircPRH1-PRR4 expression was detected by qRT-PCR in both H522 and A549 cells transfected with si-NC, si-circPRH1-PRR4#1 or si-circPRH1-PRR4#2. (b–h) Both H522 and A549 cells were transfected with si-circPRH1-PRR4 and si-NC, respectively. (b and c) Cell proliferation was investigated by cell colony formation and EdU assays. (d) Flow cytometry analysis was performed to quantify apoptotic cells. (e and f) Wound-healing and transwell invasion assays were implemented to determine cell migration and invasion, respectively. (g and h) The protein expression of MMP2 and MMP9 was detected by western blot analysis. $^*p < 0.05$

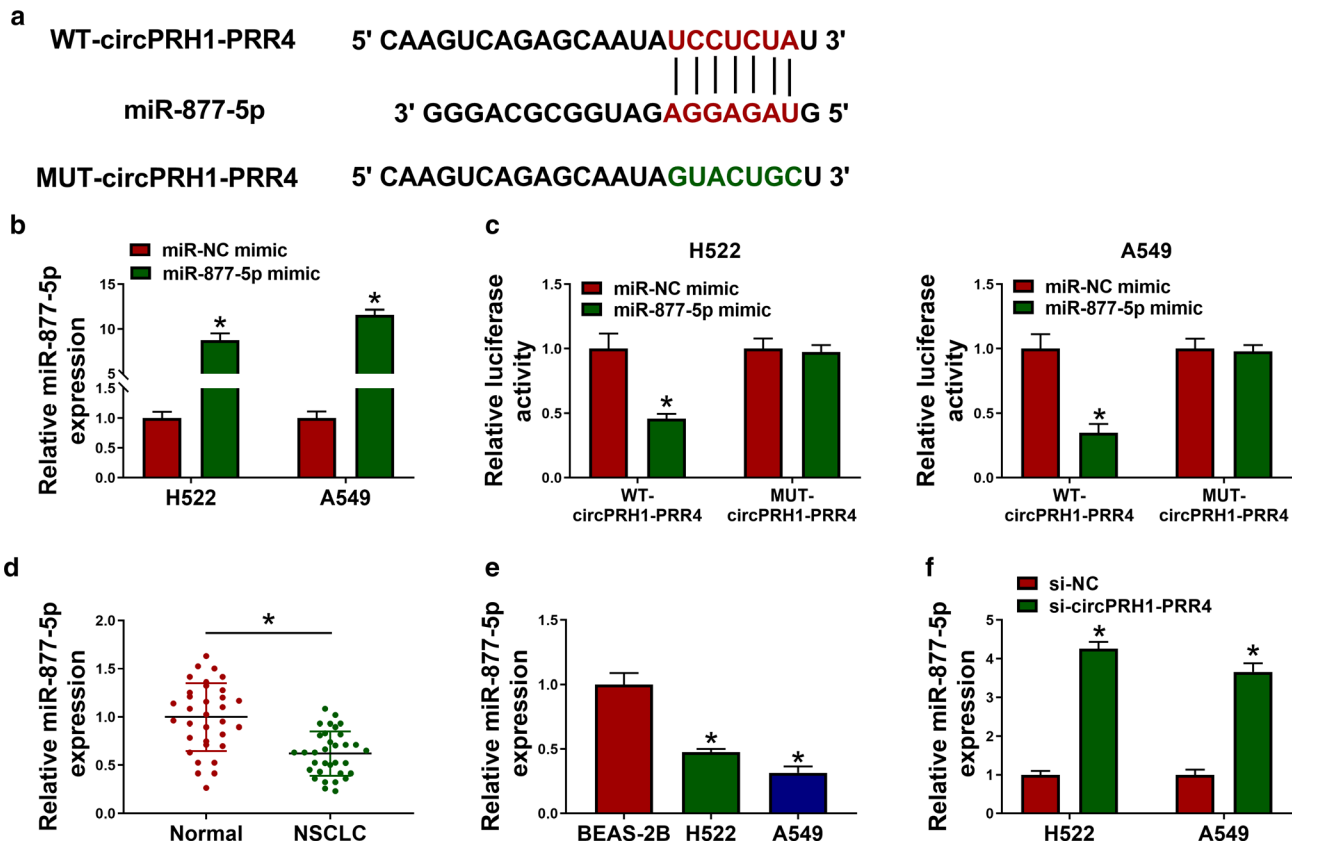

FIGURE 3 CircPRH1-PRR4 was associated with miR-877-5p. (a) The binding sites of circPRH1-PRR4 for miR-877-5p. (b) The efficiency of miR-877-5p overexpression was determined by qRT-PCR. (c) The interaction between circPRH1-PRR4 and miR-877-5p was confirmed by dual-luciferase reporter assay. (d and e) MiR-877-5p expression was checked by qRT-PCR in clinical NSCLC tissues ($N = 33$), healthy lung tissues ($N = 33$) as well as BEAS-2B, H522, and A549 cells. (f) The effect of circPRH1-PRR4 knockdown on miR-877-5p expression was confirmed by qRT-PCR. *$p < 0.05$

thickness, heated at 60°C, and deparaffinized using xylene. The sections were heated at 80°C to conduct antigen retrieval. Then, endogenous peroxidase activity was blocked by immersing the section in 0.3% hydrogen peroxide (Seebio Biotech), and the sections were incubated with anti-RAB3D (1:100; Affinity). After biotinylated secondary antibody (1:200; Affinity) was incubated with the sections, 3,3-diaminobenzidine (DAB) substrate (Phygene) was used to visualize immunoreactivity. Finally, the sections were counterstained by hematoxylin (Millipore).

Statistical analysis

The results from three independent duplicate tests were expressed as means ± standard deviations. The significant differences between the two groups were compared with Student's *t*-test or the Wilcoxon rank-sum test. One-way analysis of variance (ANOVA) with Tukey's test was employed to calculate the *p* value among three or more groups. The significant difference was compared with log-rank test in analyzing the overall survival curve of NSCLC patients. The above assessments were carried out on a GraphPad Prism software. $p < 0.05$ indicated statistical significance.

RESULTS

CircPRH1-PRR4 expression was upregulated in NSCLC tissues and cells

To figure out the role of circPRH1-PRR4 in NSCLC progression, we predicted the expression of the circRNA in NSCLC tissues through the GSE112214 dataset. The results showed that circPRH1-PRR4 expression was significantly increased in NSCLC tissues when compared with normal lung tissues (Figure 1a). We also observed high relative expression of circPRH1-PRR4 in clinical NSCLC tissues in comparison with BEAS-2B cells, as analyzed by qRT-PCR and calculated by the $2^{-\Delta\Delta Ct}$ method (Figure 1b). Additionally, we found that NSCLC patients with high expression of circPRH1-PRR4 had a poor prognosis (Figure 1c). As shown in Figure 1d, circPRH1-PRR4 expression was higher in high-metastatic NSCLC tissues than in low-metastatic NSCLC tissues (Figure 1d). The results from Figure 1e displayed the high expression of circPRH1-PRR4 in NSCLC cells (H522 and A549) in comparison with BEAS-2B cells (Figure 1e). The study found circPRH1-PRR4 expression showed little change after RNase R treatment, although the expression of linear PRH1-PRR4 was significantly reduced (Figure 1f,g), suggesting the high stability of circPRH1-PRR4. These data

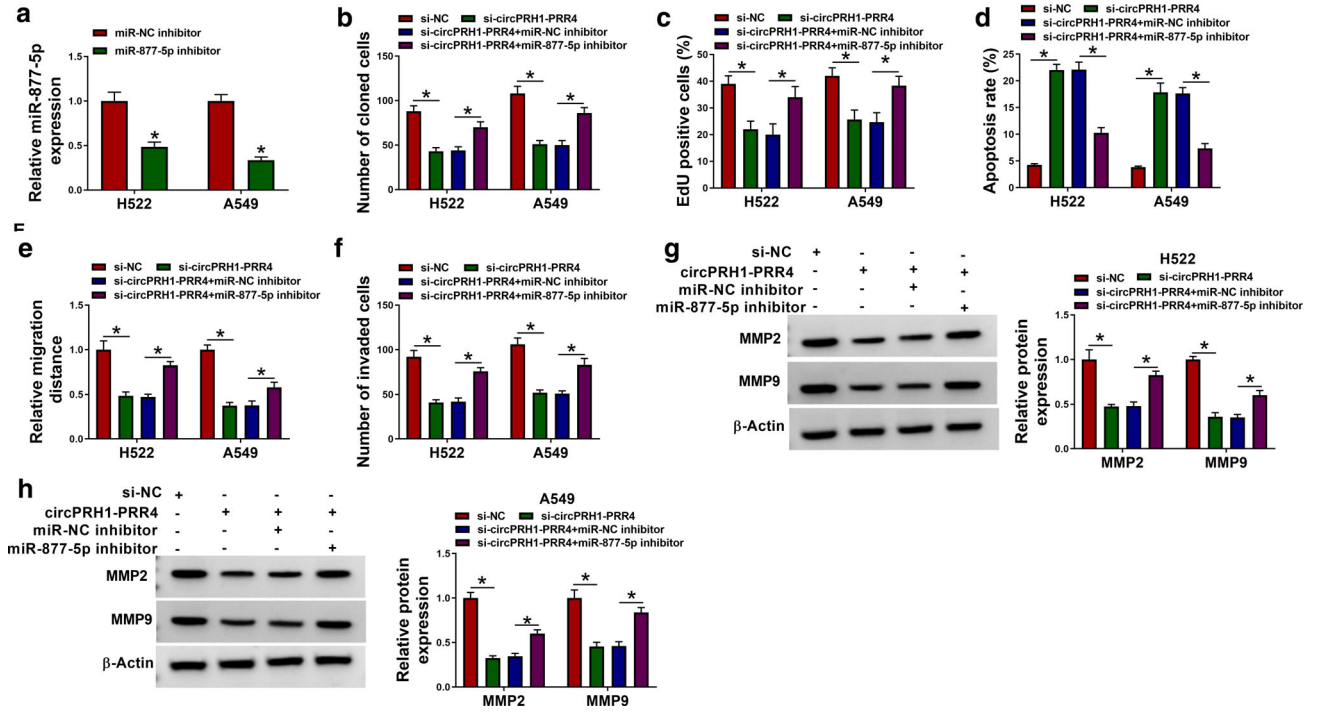

FIGURE 4 Effects of circPRH1-PRR4 depletion and miR-877-5p knockdown on NSCLC cell processes. (a) The efficiency of miR-877-5p depletion was determined by qRT-PCR. (b–h) H522 and A549 cells were transfected with si-NC, si-circPRH1-PRR4, si-circPRH1-PRR4+miR-NC inhibitor or si-circPRH1-PRR4+miR-877-5p inhibitor. (b and c) Cell colony formation and EdU assays were used to investigate cell proliferation. (d) Cell apoptotic rate was determined by flow cytometry analysis. (e and f) Cell migration and invasion were evaluated by wound-healing and transwell invasion assays, respectively. (g and h) The protein expression of MMP2 and MMP9 was checked by western blot analysis. $^*p < 0.05$

demonstrate that NSCLC development might be associated with circPRH1-PRR4 expression.

CircPRH1-PRR4 depletion inhibited cell proliferation, migration and invasion, and induced cell apoptosis in H522 and A549 cells

We silenced circPRH1-PRR4 expression to explore the consequential effects on the processes of H522 and A549 cells. Figure 2a shows that circPRH1-PRR4 expression was dramatically downregulated by si-circPRH1-PRR4#1 and si-circPRH1-PRR4#2, especially by si-circPRH1-PRR4#1. Thus, si-circPRH1-PRR4#1 (si-circPRH1-PRR4) was employed for subsequent study. Subsequently, circPRH1-PRR4 absence inhibited cell colony-forming ability and reduced the number of EdU-positive cells (Figure 2b,c), suggesting the inhibitory effect of circPRH1-PRR4 knockdown on cell proliferation. On the contrary, the apoptosis of H522 and A549 cells was induced after circPRH1-PRR4 knockdown (Figure 2d). Additionally, reduced expression of circPRH1-PRR4 weakened the migratory and invasive capacities of H522 and A549 cells (Figure 2e,f). In support, we found low expression of metastasis-related MMP2 and MMP9 after circPRH1-PRR4 silencing in both H522 and A549 cells (Figure 2g,h). Thus, all findings manifested that circPRH1-PRR4 might act as an oncogene in NSCLC.

CircPRH1-PRR4 acted as a miR-877-5p sponge in H522 and A549 cells

The study continued to explore circPRH1-PRR4-related miRNA(s). As displayed in Figure 3a, miR-877-5p carried the binding sites of circPRH1-PRR4. The high overexpression efficiency of miR-877-5p is shown in Figure 3b. It was found using dual-luciferase reporter assay that miR-877-5p mimics significantly inhibited the luciferase activity of WT-circPRH1-PRR4 rather than that of MUT-circPRH1-PRR4 (Figure 3c). This evidence confirmed the binding relationship of circPRH1-PRR4 and miR-877-5p. Comparatively, NSCLC tissues and cells (H522 and A549 cells) displayed the low expression of miR-877-5p relative to normal lung tissues or BEAS-2B cells (Figure 3d,e). To determine the association between circPRH1-PRR4 and miR-877-5p expression, qRT-PCR was performed. Data showed that miR-877-5p expression was increased after circPRH1-PRR4 knockdown (Figure 3f).

CircPRH1-PRR4 regulated NSCLC cell malignancy by binding to miR-877-5p

Given the binding relationship of circPRH1-PRR4 and miR-877-5p, we further investigated whether miR-877-5p participated in circPRH1-PRR4-mediated NSCLC cell development.

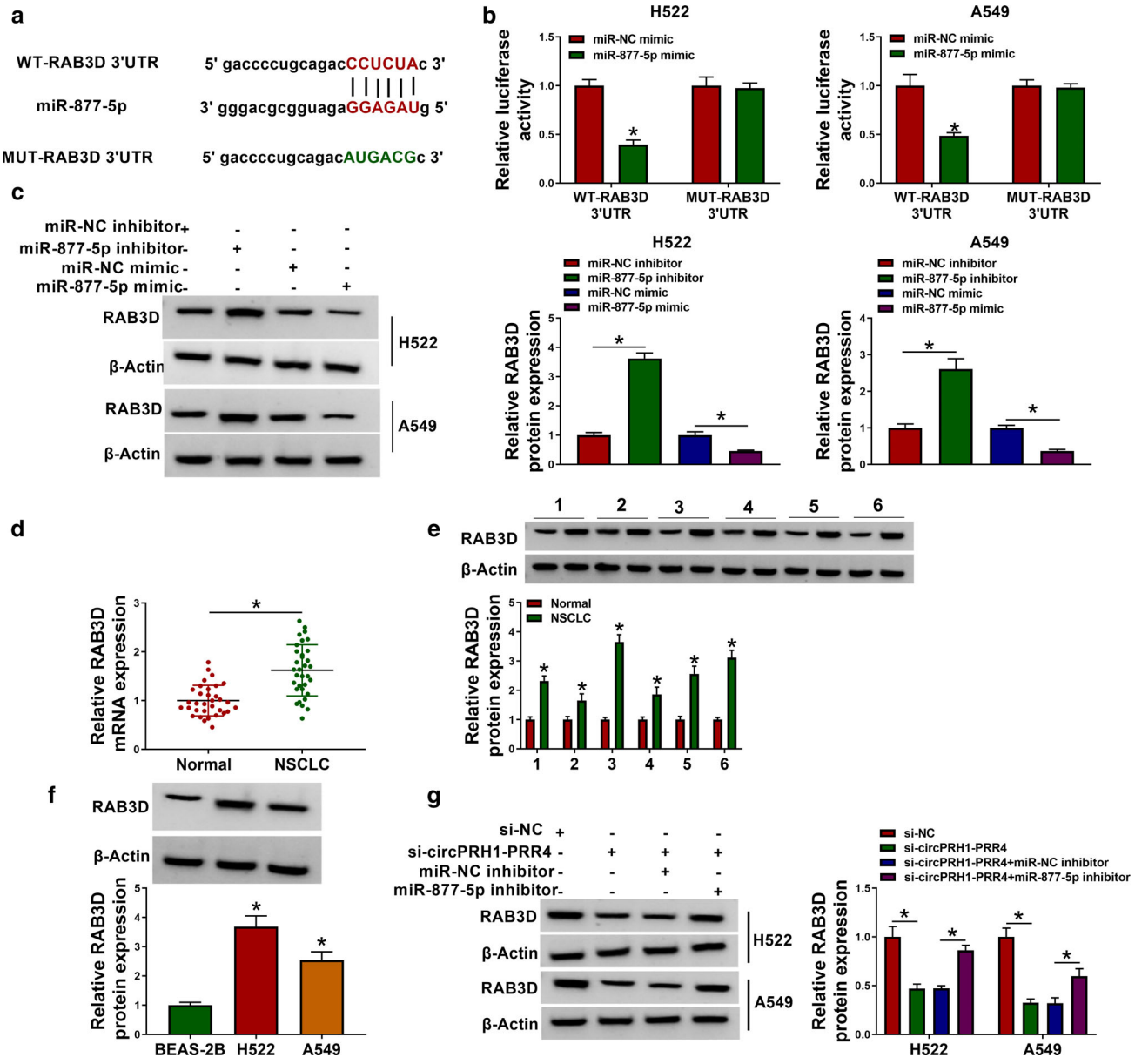

FIGURE 5 CircPRH1-PRR4 regulated RAB3D expression through miR-877-5p. (a) The binding sites of miR-877-5p for RAB3D. (b) Dual-luciferase reporter assay was employed to determine the interaction of miR-877-5p and RAB3D. (c) The impacts of miR-877-5p inhibitors and mimics on RAB3D expression were unveiled by western blot. (d–f) RAB3D expression was checked by qRT-PCR and western blot in clinical NSCLC tissues and healthy lung tissues as well as BEAS-2B, H522, and A549 cells. (g) The effects between circPRH1-PRR4 knockdown and miR-877-5p inhibitors on RAB3D protein expression were revealed by western blot. $^*p < 0.05$

The efficiency of miR-877-5p silencing was detected and is shown in Figure 4a. It was found that the repressing effect of circPRH1-PRR4 knockdown on cell proliferation was attenuated by miR-877-5p inhibitors (Figure 4b,c). Flow cytometry analysis demonstrated that the induced cell apoptosis by circPRH1-PRR4 depletion was remitted after transfection of miR-877-5p inhibitor (Figure 4d). In line with the above data, the inhibitory impacts of circPRH1-PRR4 absence on cell migration and invasion were rescued after miR-877-5p depletion (Figure 4e,f). In support, miR-877-5p inhibitors also attenuated circPRH1-PRR4 knockdown-mediated inhibition of MMP2 and MMP9 expression (Figure 4g,h). All these findings contribute to explain the relationship of circPRH1-PRR4 and miR-877-5p in regulating NSCLC cell malignancy.

CircPRH1-PRR4 modulated RAB3D by interacting with miR-877-5p in H522 and A549 cells

The mRNA associated with miR-877-5p was screened. As shown in Figure 5a,b, RAB3D carried the binding sites of miR-877-5p, and miR-877-5p mimics significantly reduced the luciferase activity of WT-RAB3D 3′UTR rather than that

of MUT-RAB3D 3′UTR, suggesting the binding relationship of miR-877-5p and RAB3D. Thus, RAB3D was employed as a follow-up subject. Then, we found that miR-877-5p inhibitors increased RAB3D expression and miR-877-5p mimics decreased RAB3D expression (Figure 5c). The data from Figure 5d,f show that RAB3D expression is upregulated in NSCLC tissues and cells (H522 and A549) as compared with healthy lung tissues and BEAS-2B cells, respectively. Importantly, western blot analysis showed that the reduced expression of RAB3D by circPRH1-PRR4 knockdown was relieved after miR-877-5p depletion (Figure 5g). These data manifested that circPRH1-PRR4 regulated RAB3D expression by miR-877-5p.

RAB3D overexpression remitted the effects of miR-877-5p on NSCLC cell processes

Having proved that RAB3D was a target mRNA of miR-877-5p, we continued to explore whether miR-877-5p regulated NSCLC cell malignancy by targeting RAB3D. To establish this, we overexpressed miR-877-5p and RAB3D to determine the consequential effects on the processes of H522 and A549 cells. Western blot data initially ascertained the efficiency of RAB3D overexpression (Figure 6a). Then, we found that miR-877-5p mimics inhibited cell proliferation, but induced cell apoptosis; however, these effects were attenuated by RAB3D introduction (Figure 6b, d). Additionally, miR-877-5p mimics inhibited cell migration and invasion, which was restored by enforced expression of RAB3D (Figure 6e,f). In support, reduced expression of MMP2 and MMP9 caused by miR-877-5p was remitted after RAB3D overexpression (Figure 6g–i). Taken together, these data explained that miR-877-5p inhibited NSCLC progression by interacting with RAB3D in vitro.

CircPRH1-PRR4 knockdown inhibited A549 cell malignancy *in vivo*

An in vivo experiment was used to confirm the data about the inhibitory effect of circPRH1-PRR4 silencing on NSCLC cell malignancy in vitro. As shown in Figure 7a,b, circPRH1-PRR4 silencing inhibited the volume and weight of neoplasms as compared with control groups. Additionally, circPRH1-PRR4 absence downregulated the expression of circPRH1-PRR4 and RAB3D, and upregulated miR-877-5p (Figure 7c–e). Comparatively, the positive expression rate of RAB3D was lower in the neoplasms from the sh-circPRH1-PRR4 group than in tissues from the sh-NC group (Figure 7f). In addition, we found that miR-877-5p depletion or RAB3D overexpression relieved circPRH1-PRR4 knockdown-induced inhibition of tumor

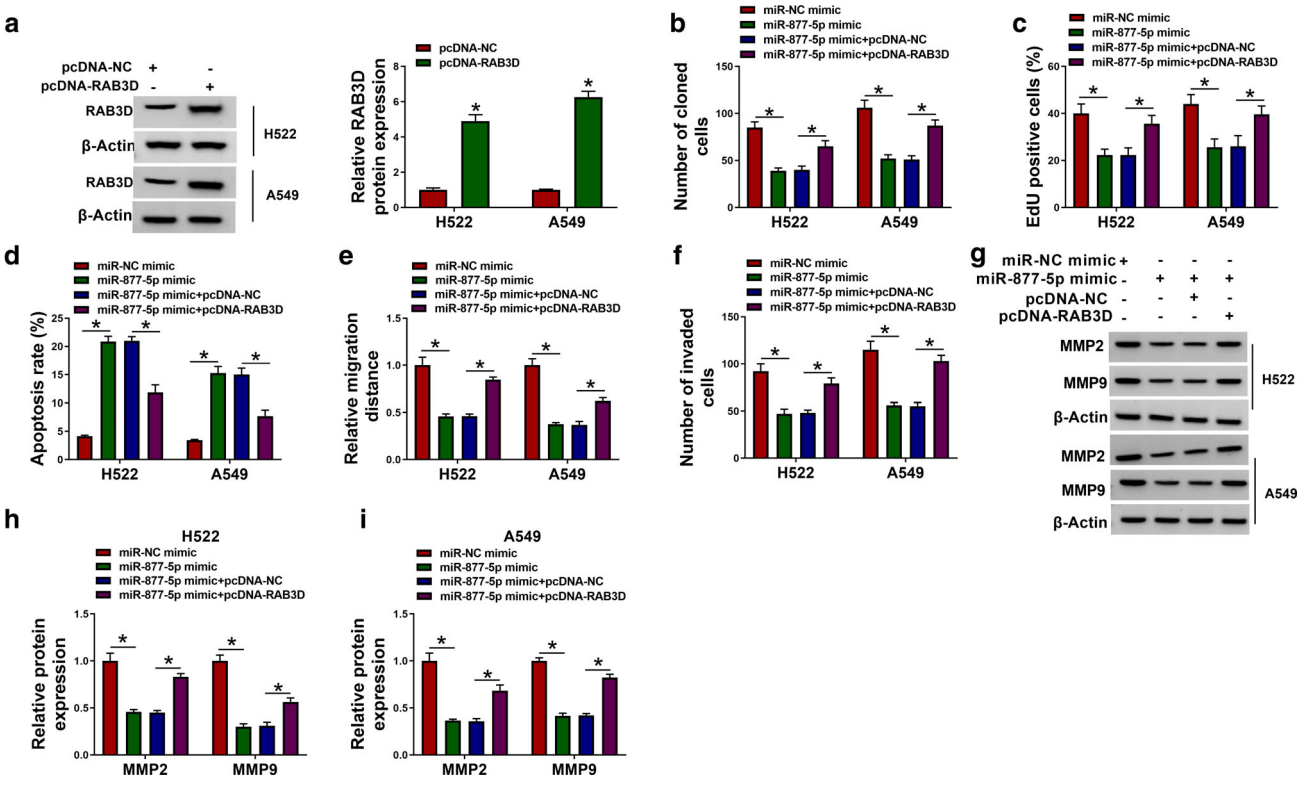

FIGURE 6 MiR-877-5p regulated NSCLC cell malignancy by binding to RAB3D. (a) The efficiency of RAB3D overexpression was detected by western blot. (b–i) H522 and A549 cells were transfected with miR-NC mimic, miR-877-5p mimic, miR-877-5p mimic+pcDNA-NC or miR-877-5p mimic+pcDNA-RAB3D, and cell proliferation was detected by cell colony formation and EdU assays (b and c), cell apoptosis by flow cytometry analysis (d), cell migration by wound-healing assay (e), cell invasion by transwell invasion assay (f) as well as MMP2 and MMP9 expression by western blot analysis (g–i). $^*p < 0.05$

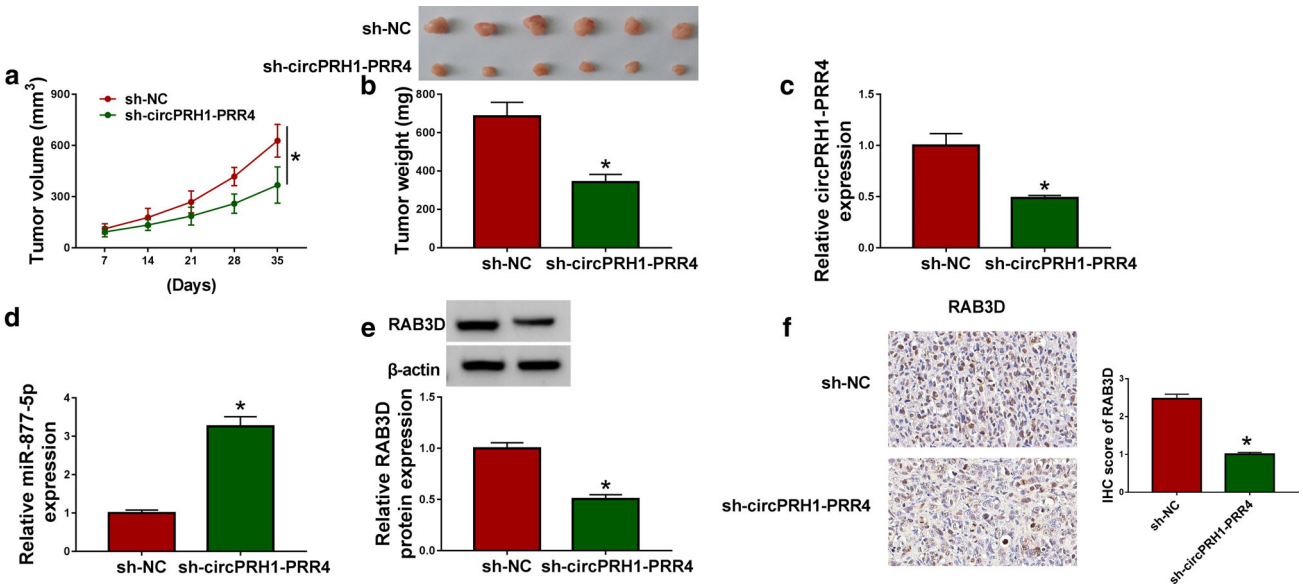

FIGURE 7 The effect of circPRH1-PRR4 silencing on A549 cell malignancy. (a and b) The effects of circPRH1-PRR4 silencing on tumor volume and weight. (c and d) CircPRH1-PRR4 and miR-877-5p expression were detected by qRT-PCR in the neoplasms from sh-circPRH1-PRR4 and sh-NC groups. (e) Western blot analysis was employed to check RAB3D protein expression in the neoplasms from sh-circPRH1-PRR4 and sh-NC groups. (f) The positive expression rate of RAB3D was determined by IHC assay in the neoplasms from sh-circPRH1-PRR4 and sh-NC groups. *$p < 0.05$

tumorigenesis (Supporting Information Figure S1). Collectively, the above data demonstrated that circPRH1-PRR4 absence inhibited A549 cell malignancy.

DISCUSSION

With the usage of advanced computational methods like the Locality-Constrained Linear Coding algorithm, multiple circRNAs have been revealed to be associated with cancers, and thus can been used as therapeutic targets.[3,4] However, there are challenges hindering the application of circRNAs as biomarkers. For example, evaluating biomarkers needs multiple prospective studies before circRNA is recommended for clinical use. Larger-scale repeated tests to choose the optimal concentration for its application to be compatible with the needs of patients are needed. A study unveiling the underlying mechanism of circRNA in regulating NSCLC malignant progression is absent. More understanding regarding the issue will be helpful to develop an effective therapeutic target for NSCLC. In the present study, we revealed the role of circPRH1-PRR4 in NSCLC progression. The study identified the high expression of circPRH1-PRR4 in clinical NSCLC tissues and cells, and found circPRH1-PRR4 knockdown impeded NSCLC cell malignancy in vitro and in vivo. Importantly, we provided evidence that the function of circPRH1-PRR4 in NSCLC development was associated with miR-877-5p and RAB3D.

As reported, the role of some circRNAs has been revealed in NSCLC progression. For instance, circ_101237 stimulated mitogen-activated protein kinase 1 (MAPK1) in an miR-490-3p-dependent manner, thereby contributing to the proliferation and metastasis of NSCLC cells.[5] Circ_103993 absence hindered cell proliferation and induced cell apoptosis by miR-1271.[6] Circ_0002483 introduction weakened cell proliferative and invasive ability via absorbing miR-182-5p to release the repression on several mRNAs, such as forkhead box O1 (FOXO1) and FOXO3, in vitro.[7] This evidence suggests the oncogenic or tumor-repressing role of circRNA in NSCLC progression. The data considered also demonstrated that circPRH1-PRR4 overexpression was associated with poor clinical outcomes of NSCLC patients, and knockdown of the circRNA relieved hypoxia-caused NSCLC cell growth, glycolysis, and metastasis.[8] In this work, we found high expression of circPRH1-PRR4 in NSCLC specimens and cells, and circPRH1-PRR4 knockdown inhibited cell proliferation and motility, which were consistent with the previous data.[9] Different from the published literature, our results also manifested that circPRH1-PRR4 mediated NSCLC progression by inhibiting cell apoptosis. In addition, we proved the inhibitory role of circPRH1-PRR4 knockdown in NSCLC cell malignancy using mouse model assay based on the finding that circPRH1-PRR4 silencing inhibited tumor volume and weight.

The miRNA able to bind to circPRH1-PRR4 was explored. According to bioinformatics predictions, miR-877-5p was employed as a candidate. MiR-877-5p, a cancer-related miRNA, has been revealed to have a tumor-repressing role in glioblastoma,[10] cervical cancer,[11] laryngeal squamous cell carcinoma,[12] hepatocellular carcinoma,[13] and gastric cancer.[14] In particular, Du and his colleagues

indicated that miR-877-5p inhibited NSCLC cell malignancy by regulating cell proliferation, metastasis, and apoptosis.[15] This evidence indicates that miR-877-5p has potential as a target miRNA of circPRH1-PRR4. As expected, it was validated that circPRH1-PRR4 acts as a sponge for miR-877-5p using a dual-luciferase reporter assay. Additionally, NSCLC tissues and cells displayed low expression of miR-877-5p compared with control groups. Also, miR-877-5p was negatively regulated by circPRH1-PRR4 in vivo and in vitro, and its inhibitors were able to relieve circPRH1-PRR4 knockdown-mediated action.

RAB3D, as a member of the Ras-like small GTPase family, regulates vesicle trafficking between the trans-Golgi network and the plasma membrane.[16] The protein is defined as a secretory protein and has a key part in cancer progression. It has been reported that RAB3D promotes cell proliferation and metastasis of colorectal cancer,[17] squamous cell carcinoma,[18] and melanoma.[19] RAB3D overexpression was also closely associated with tumor-node-metastasis staging not grade, and RAB3D expression was much higher in tissues of some cancers, such as breast cancer, lung cancer, and liver cancer, compared with healthy tissues,[20] which implies that RAB3D is able to refer the sufferers for diagnosis and treatment. In this report, RAB3D was confirmed as a target mRNA of miR-877-5p, and negatively modulated by miR-877-5p. Additionally, it was found that RAB3D was augmented in NSCLC tissues, and promoted cell proliferation and aggressiveness, but inhibited cell apoptosis, which was supported by the previous paper.[21] Meanwhile, RAB3D was upregulated in NSCLC cells in comparison with controls. More importantly, the study ascertained that circPRH1-PRR4 regulated RAB3D expression by absorbing miR-877-5p.

However, there were limitations to this study due to our current laboratory conditions. First, the effect of circPRH1-PRR4 on miR-877-5p/RAB3D axis in vivo was not explored in the present study. Additionally, in vivo data explaining the impact of circPRH1-PRR4/miR-877-5p/RAB3D axis on tumor metastasis were absent. We intend to design a series of experiments to solve the above problems to improve the mechanism behind circPRH1-PRR4 modulating NSCLC.

Taken together, NSCLC malignant progression might involve high expression of circPRH1-PRR4 and the molecular mechanism responsible for circPRH1-PRR4-mediated NSCLC progression was that circPRH1-PRR4 sponged miR-877-5p to release the inhibition on RAB3D expression. This finding makes circPRH1-PRR4 an attractive candidate for NSCLC therapy.

ACKNOWLEDGMENTS

None.

CONFLICT OF INTEREST

The authors declare that they have no conflicts of interest.

ORCID

Quanxing Li https://orcid.org/0000-0002-7077-4568

REFERENCES

1. Siegel RL, Miller KD, Jemal A. Cancer statistics, 2018. CA Cancer J Clin. 2018;68:7–30.
2. Bray F, Ferlay J, Soerjomataram I, Siegel RL, Torre LA, Jemal A. Global cancer statistics 2018: GLOBOCAN estimates of incidence and mortality worldwide for 36 cancers in 185 countries. CA Cancer J Clin. 2018;68:394–424.
3. Wang Y, Zhang Y, Wang P, Fu X, Lin W. Circular RNAs in renal cell carcinoma: implications for tumorigenesis, diagnosis, and therapy. Mol Cancer. 2020;19:149.
4. Zhao Q, Yang Y, Ren G, Ge E, Fan C. Integrating bipartite network projection and KATZ measure to identify novel CircRNA-disease associations. IEEE Trans Nanobioscience. 2019;18:578–84.
5. Zhang ZY, Gao XH, Ma MY, Zhao CL, Zhang YL, Guo SS. CircRNA_101237 promotes NSCLC progression via the miRNA-490-3p/MAPK1 axis. Sci Rep. 2020;10:9024.
6. Lv YS, Wang C, Li LX, Han S, Li Y. Effects of circRNA_103993 on the proliferation and apoptosis of NSCLC cells through miR-1271/ERG signaling pathway. Eur Rev Med Pharmacol Sci. 2020;24:8384–93.
7. Li X, Yang B, Ren H, Xiao T, Zhang L, Li L, et al. Hsa_circ_0002483 inhibited the progression and enhanced the taxol sensitivity of non-small cell lung cancer by targeting miR-182-5p. Cell Death Dis. 2019;10:953.
8. Li C, Liu H, Niu Q, Gao J. Circ_0000376, a novel circRNA, promotes the progression of non-small cell lung cancer through regulating the miR-1182/NOVA2 network. Cancer Manag Res. 2020;12:7635–47.
9. Sun H, Chen Y, Fang YY, Cui TY, Qiao X, Jiang CY, et al. Circ_0000376 enhances the proliferation, metastasis, and chemoresistance of NSCLC cells via repressing miR-384. Cancer Biomark. 2020;29:463–73.
10. Xie H, Shi S, Chen Q, Chen Z. LncRNA TRG-AS1 promotes glioblastoma cell proliferation by competitively binding with miR-877-5p to regulate SUZ12 expression. Pathol Res Pract. 2019;215:152476.
11. Liang J, Zhang S, Wang W, Xu Y, Kawuli A, Lu J, et al. Long non-coding RNA DSCAM-AS1 contributes to the tumorigenesis of cervical cancer by targeting miR-877-5p/ATXN7L3 axis. Biosci Rep. 2020;40:BSR20192061.
12. Wang X, Liu L, Zhao W, Li Q, Wang G, Li H. LncRNA SNHG16 promotes the progression of laryngeal squamous cell carcinoma by mediating miR-877-5p/FOXP4 axis. Onco Targets Ther. 2020;13:4569–79.
13. Pafundi PC, Caturano A, Franci G. Comment on: MiR-877-5p suppresses cell growth, migration and invasion by targeting cyclin dependent kinase 14 and predicts prognosis in hepatocellular carcinoma. Eur Rev Med Pharmacol Sci. 2018;22:4401–2.
14. Guo T, Wang W, Ji Y, Zhang M, Xu GY, Lin S. LncRNA PROX1-AS1 facilitates gastric cancer progression via miR-877-5p/PD-L1 Axis. Cancer Manag Res. 2021;13:2669–80.
15. Du LJ, Mao LJ, Jing RJ. Long noncoding RNA DNAH17-AS1 promotes tumorigenesis and metastasis of non-small cell lung cancer via regulating miR-877-5p/CCNA2 pathway. Biochem Biophys Res Commun. 2020;533:565–72.
16. Stenmark H. Rab GTPases as coordinators of vesicle traffic. Nat Rev Mol Cell Biol. 2009;10:513–25.
17. Luo Y, Yu SY, Chen JJ, Qin J, Qiu YE, Zhong M, et al. MiR-27b directly targets Rab3D to inhibit the malignant phenotype in colorectal cancer. Oncotarget. 2018;9:3830–41.
18. Zhang J, Kong R, Sun L. Silencing of Rab3D suppresses the proliferation and invasion of esophageal squamous cell carcinoma cells. Biomed Pharmacother. 2017;91:402–7.
19. Xie J, Zheng Y, Xu X, Sun C, Lv M. Long noncoding RNA CAR10 contributes to melanoma progression by suppressing miR-125b-5p to induce RAB3D expression. Onco Targets Ther. 2020;13:6203–11.
20. Yang J, Liu W, Lu X, Liu W, Lu X, Fu Y, et al. High expression of small GTPase Rab3D promotes cancer progression and metastasis. Oncotarget. 2015;6:11125–38.

21. Li L, Wan K, Xiong L, Liang S, Tou F, Guo S. CircRNA hsa_circ_0087862 acts as an oncogene in non-small cell lung cancer by targeting miR-1253/RAB3D axis. Onco Targets Ther. 2020;13: 2873–86.

SUPPORTING INFORMATION

Additional supporting information may be found in the online version of the article at the publisher's website.

How to cite this article: Ma J, Li Q, Li Y. CircRNA PRH1-PRR4 stimulates RAB3D to regulate the malignant progression of NSCLC by sponging miR-877-5p. Thorac Cancer. 2022;13:690–701. https://doi.org/10.1111/1759-7714.14264